

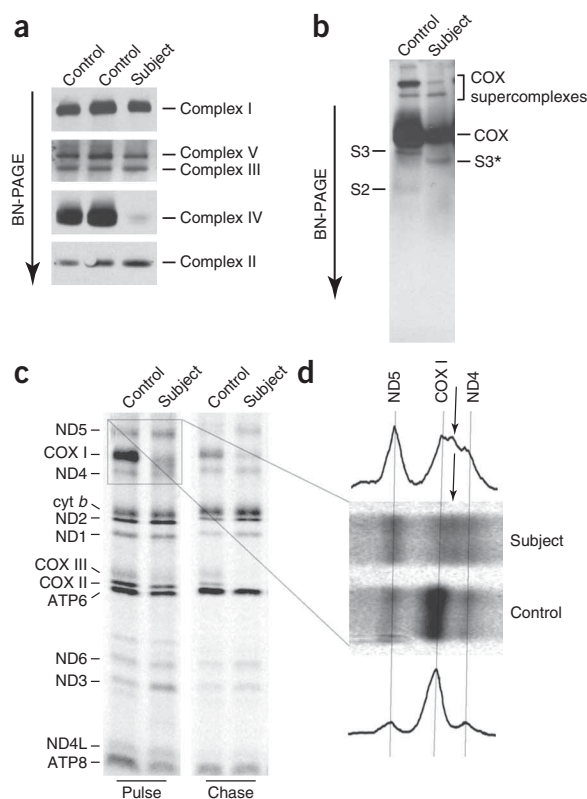
Mutation in *TACO1*, encoding a translational activator of COX I, results in cytochrome *c* oxidase deficiency and late-onset Leigh syndrome

Woranontee Weraarpachai^{1,2,8}, Hana Antonicka^{2,8}, Florin Sasarman^{1,2}, Jürgen Seeger³, Bertold Schrank⁴, Jill E Kolesar², Hanns Lochmüller^{5,7}, Mario Chevrette⁶, Brett A Kaufman², Rita Horvath^{5,7} & Eric A Shoubridge^{1,2}

Defects in mitochondrial translation are among the most common causes of mitochondrial disease¹, but the mechanisms that regulate mitochondrial translation remain largely unknown. In the yeast *Saccharomyces cerevisiae*, all mitochondrial mRNAs require specific translational activators, which recognize sequences in 5' UTRs and mediate translation². As mammalian mitochondrial mRNAs do not have significant 5' UTRs³, alternate mechanisms must exist to promote translation. We identified a specific defect in the synthesis of the mitochondrial DNA (mtDNA)-encoded COX I subunit in a pedigree segregating late-onset Leigh syndrome and cytochrome *c* oxidase (COX) deficiency. We mapped the defect to chromosome 17q by functional complementation and identified a homozygous single-base-pair insertion in *CCDC44*, encoding a member of a large family of hypothetical proteins containing a conserved DUF28 domain. *CCDC44*, renamed *TACO1* for translational activator of COX I, shares a notable degree of structural similarity with bacterial homologs⁴, and our findings suggest that it is one of a family of specific mammalian mitochondrial translational activators.

Figure 1 Compromised assembly of COX and impaired synthesis of COX subunit I in subject fibroblasts. (a) BN-PAGE analysis of fibroblasts from the affected individual and two controls. Antibodies against individual subunits of OXPHOS complexes I–V were used for immunoblotting (see Online Methods). (b) BN-PAGE immunoblot analysis with an antibody against COX subunit IV; S3* is a newly identified COX subcomplex in subject fibroblasts. (c) Pulse-chase labeling of newly synthesized mitochondrial polypeptides (indicated on the left; ND, subunits of complex I; COX, subunits of complex IV; cyt *b*, subunit of complex III; ATP, subunits of complex V) in subject and control fibroblasts. (d) Magnification of the boxed region from c and a line graph of the intensities of individual bands. The arrows indicate a shorter version of the COX I polypeptide in the subject.

The index subject (pedigree, **Supplementary Fig. 1** online), presented with childhood-onset and slowly progressive Leigh syndrome due to an isolated COX deficiency (**Supplementary Note** online).



¹Department of Human Genetics, McGill University, Montreal, Quebec, Canada. ²Montreal Neurological Institute, McGill University, Montreal, Quebec, Canada. ³Department of Pediatrics, Deutsche Klinik für Diagnostik GmbH, Wiesbaden, Germany. ⁴Department of Neurology, Deutsche Klinik für Diagnostik GmbH, Wiesbaden, Germany. ⁵Friedrich-Baur Institute, Ludwig-Maximilians-University, Munich, Germany. ⁶Department of Surgery, Urology Division, McGill University and The Research Institute of the McGill University Health Centre, Montreal, Quebec, Canada. ⁷Present addresses: Institute of Human Genetics, Newcastle University, Newcastle, UK (H.L.) and Mitochondrial Research Group, Newcastle University, Newcastle, UK (R.H.). ⁸These authors contributed equally to this work. Correspondence should be addressed to E.A.S. (eric@ericpc.mni.mcgill.ca).

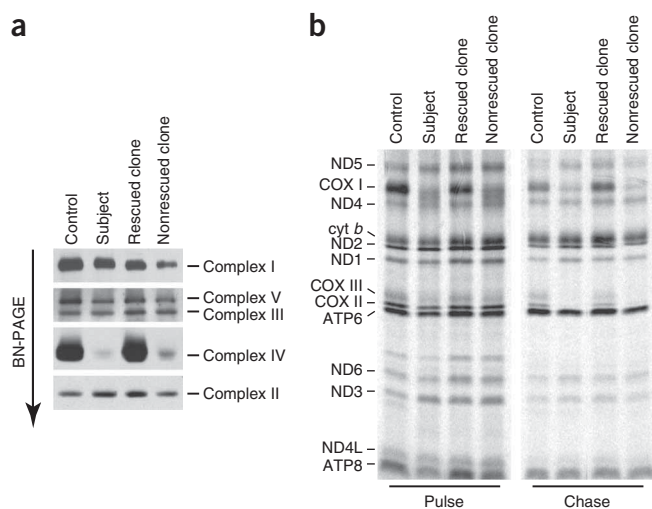


Figure 2 The biochemical defect in subject fibroblasts is rescued by microcell-mediated transfer of chromosome 17q. **(a,b)** BN-PAGE **(a)** and pulse labeling **(b)** of mitochondrial polypeptides in control and subject fibroblasts, and in one rescued and one nonrescued clone, obtained after the transfer of the q-arm of chromosome 17 into subject fibroblasts. Complex I–V, OXPHOS complexes; ND, subunits of complex I; COX, subunits of complex IV; cyt *b*, subunit of complex III; ATP, subunits of complex V.

Blue-Native polyacrylamide gel electrophoresis (BN-PAGE) analysis of subject fibroblasts showed greatly reduced steady-state levels of fully assembled COX (**Fig. 1a**), but normal levels of the other respiratory chain complexes. No previously described COX subcomplexes were present in the fibroblasts from the subject; however, we detected a very small amount of a ~135-kDa subcomplex (S3*) (**Fig. 1b**), containing at least subunits II, IV and VIc (**Supplementary Fig. 2** online).

To determine whether the rates of synthesis and turnover of the individual mtDNA-encoded COX subunits were altered, we pulse-labeled then chased the mitochondrial translation products in subject fibroblasts. We found a specific defect in the rate of synthesis of the COX I subunit (**Fig. 1c**), which was reduced by approximately 65%. The remaining radiolabeled material appeared as a smear of apparently truncated COX I polypeptides, with one main premature translation product (**Fig. 1d**). The rates of synthesis of the other mitochondrially encoded polypeptides were similar to control in most cases (data not shown), although there was a consistent ~50–80% increase in some of the ND subunits, and in cyt *b*. Although the synthesis of COX III was decreased in the experiment shown (**Fig. 1c**), this was not a consistent result. The compromised synthesis of COX I, and the consequent reduction in assembled COX, resulted in an increased degradation of all newly synthesized COX subunits. COX II and III were practically undetectable at the end of the chase period (less than 15% of control), whereas 37% of control COX I could be detected, representing only the full-length polypeptide (**Fig. 1c**).

A nuclear origin of the defect was confirmed by fusion of the subject's fibroblasts with human (143B) rho⁰ cells (data not shown), and we found no evidence for mtDNA depletion or large-scale mtDNA deletions (data not shown). Sequence analysis of the *MTCO1* gene identified no mutations, and RNA blot analysis of mitochondrial transcripts showed normal transcript levels for all mtDNA-encoded COX subunits (**Supplementary Fig. 3** online), as well as for two subunits of complex I and both ribosomal subunits, demonstrating that the COX I synthesis defect was not due to a decreased amount of COX I mRNA, but rather to a mutation in a factor specifically responsible for COX I translation. Overexpression of 14 different known COX assembly factors (see Online Methods) did not rescue the defect (data not shown).

Genome-wide linkage analysis using microsatellite markers showed significant linkage to chromosome 17 with a maximum lod score of 3.3 at D17S2193 (data not shown), but did not lead to identification of the gene defect. Using microcell-mediated chromosome transfer, we found that transfer of a copy of chromosome 17q into subject fibroblasts rescued the biochemical defect in 40 of 46 independent clones (**Fig. 2**). Copy number analysis of two rescuing and two nonrescuing clones using an SNP-chip array identified two regions on chromosome 17q (49.1–53.1 Mb and 58.5–64.2 Mb) present exclusively in the rescuing clones (**Supplementary Fig. 4** online). These two regions encompass 103 genes, five of which were predicted to encode mitochondrial proteins (**Supplementary Table 1** online) by independent mitochondrial targeting prediction programs (Predotar, Target P, MitoPred, MitoProt and MitoPWolf).

Sequence analysis of the cDNA for *CCDC44* (coil-coiled domain-containing protein 44) from the subject fibroblasts detected a homozygous one-base-pair insertion at position 472 (472insC), resulting in a frameshift and the creation of a premature stop codon (**Fig. 3a,b**). We confirmed the presence of this mutation in the genomic DNA from subject fibroblasts by restriction enzyme analysis (**Fig. 3c**). Steady-state concentrations of *CCDC44* mRNA were greatly reduced in subject fibroblasts, as predicted by the presence of a premature stop codon and consequent nonsense-mediated RNA decay (**Fig. 3d**). The mutation was absent in 100 unrelated controls, and segregated as

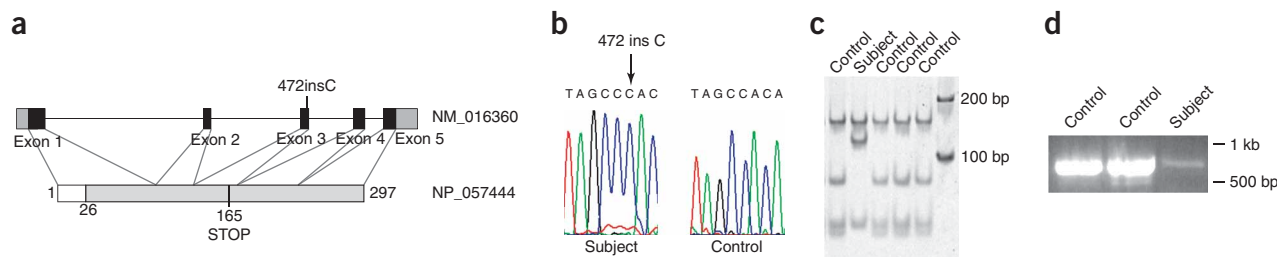


Figure 3 Mutational analysis of *TACO1* in the index subject. **(a)** Schematic diagram of *TACO1* gene and protein. Positions of the mutation in the subject DNA and the resulting premature stop codon are indicated. Dark boxes in *TACO1* gene denote the coding regions; gray boxes denote 5' and 3' UTRs. White box in *TACO1* protein indicates the predicted mitochondrial leader sequence. **(b)** Sequencing analysis of exon 3 of *TACO1* indicating the position of the homozygous 472insC insertion in the affected individual. **(c)** RFLP analysis of exon 3 of *TACO1* amplified from genomic DNA of the affected individual and four controls and digested with MwoI. **(d)** RT-PCR of the full-length *TACO1* cDNA from two controls and subject fibroblasts.

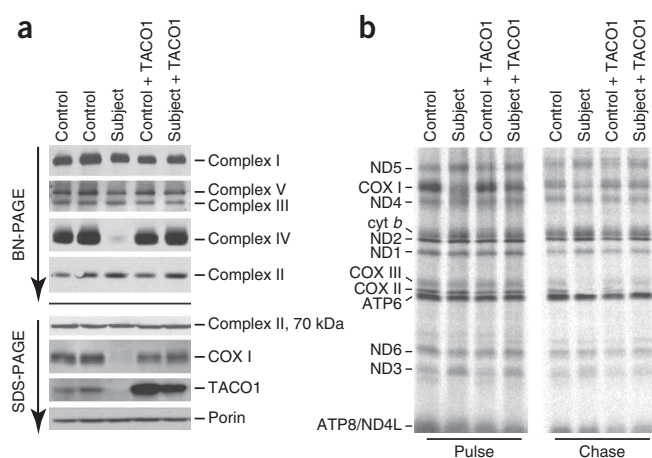


Figure 4 Overexpression of TACO1 rescues the mitochondrial translation defect and the COX assembly defect in subject fibroblasts. **(a)** BN-PAGE analysis of the assembly of individual OXPHOS complexes in control and subject fibroblasts overexpressing TACO1 protein (upper panel). Immunoblot analysis of COX I and TACO1 steady-state levels. Porin and the complex II 70-kDa subunit were used as loading controls (lower panel). **(b)** The mitochondrial translation products were pulse-labeled then chased in control and subject fibroblasts alone, and in cells overexpressing TACO1. ND, subunits of complex I; COX, subunits of complex IV; cyt *b*, subunit of complex III; ATP, subunits of complex V.

expected in the pedigree; all affected individuals carried the homozygous mutation, whereas unaffected individuals were either heterozygous (both parents) or homozygous for the wild-type sequence (**Supplementary Fig. 1**). We named this protein TACO1 for translational activator of mitochondrially encoded COX I.

Expression of wild-type TACO1 in subject fibroblasts rescued the COX assembly defect (**Fig. 4a**), the COX I synthesis defect (**Fig. 4b**) and COX activity (104% of control). TACO1 was undetectable by immunoblot analysis of mitochondria isolated from subject fibroblasts using polyclonal antibodies directed against both N- and C-terminal peptide sequences (**Fig. 4a**). The cDNA for TACO1 encodes a protein of 297 amino acids, with a predicted mitochondrial presequence of 26 amino acids, which would produce a 29.8-kDa mature protein. A C-terminal hemagglutinin-tagged version of TACO1 expressed in HEK293 cells localized to mitochondria by immunocytochemistry (**Fig. 5a**), and alkaline carbonate extraction of isolated mitochondria showed that it behaves as a mitochondrial matrix protein (**Fig. 5b**).

To test whether TACO1 associates with other mitochondrial proteins, we separated native complexes present in mitochondria from control fibroblasts cells by size exclusion. Immunoblot analysis of the individual fractions identified the majority of TACO1 protein in a higher molecular weight complex of about 74 kDa (**Fig. 5c**), indicating that TACO1 either functions as a multimer or is in a complex with another protein(s). We found a very similar elution pattern using an antibody to mitochondrial translation elongation factor Ts (EFTs), but not mitochondrial translation elongation factor Tu (EFTu), suggesting a potential interaction between mitochondrial translation factor(s) and TACO1. Overexpression of a C-terminal hemagglutinin-tagged version of the protein in control and subject fibroblasts, which resulted in substantially higher steady-state levels of TACO1-hemagglutinin compared to the endogenous protein, decreased translation of all mitochondrial polypeptides (**Fig. 6**) and

the assembly of all respiratory chain complexes (**Supplementary Fig. 5** online), suggesting that TACO1 interacts with a common element of the mitochondrial translation apparatus that can be titrated out. This effect was not simply due to the presence of the hemagglutinin tag, as the tagged construct was as effective as the wild-type cDNA at rescuing the translation defect when expressed at appropriate levels. Although we were able to immunoprecipitate TACO1-hemagglutinin using an antibody to hemagglutinin, it did not coimmunoprecipitate with EFTs (or EFTu, EFG1) (data not shown), which indicates that if TACO1 does interact with translation elongation factors, the proteins do not form a stable complex.

The *S. cerevisiae* TACO1 ortholog, YGR021w, is 29% identical and 43% similar to the human protein; however, mitochondrial translation experiments on the *ygr021wΔ* deletion strain did not show any translation defects (**Supplementary Fig. 6a** online). Furthermore, the COX activity of *ygr021wΔ* mutant cells grown on either glycerol or galactose was 70–100% of control, whereas that of the *shy1Δ* mutant, in which a known COX assembly factor is deleted, was less than 5% of controls when grown on galactose. The *ygr021wΔ* strain also grows on nonfermentable carbon sources, even acetate, with a similar doubling time as control strains (data not shown), and is respiratory-competent as indicated by TTC overlay (**Supplementary**

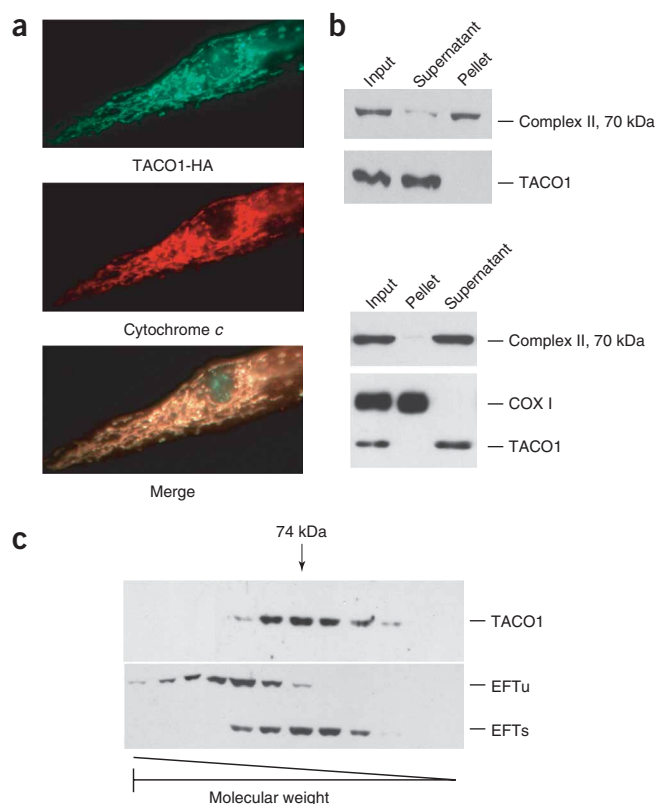


Figure 5 TACO1 is a mitochondrial matrix protein. **(a)** Immunocytochemistry of HEK293 cells transfected with TACO1-HA. Antibodies to hemagglutinin and cytochrome *c* were used as indicated. **(b)** SDS-PAGE immunoblot analysis of sonicated mitochondria (upper panel) and alkaline carbonate extracts of mitochondria (lower panel) from control fibroblasts using antibodies against TACO1, the 70-kDa subunit of complex II and COX subunit I (COX I). **(c)** Mitochondria isolated from control fibroblasts were separated on a size exclusion column and individual fractions were run on SDS-PAGE and immunoblotted with antibodies against TACO1 and EFTu/Ts. The molecular weight of individual fractions was determined by calibration of the size exclusion column.

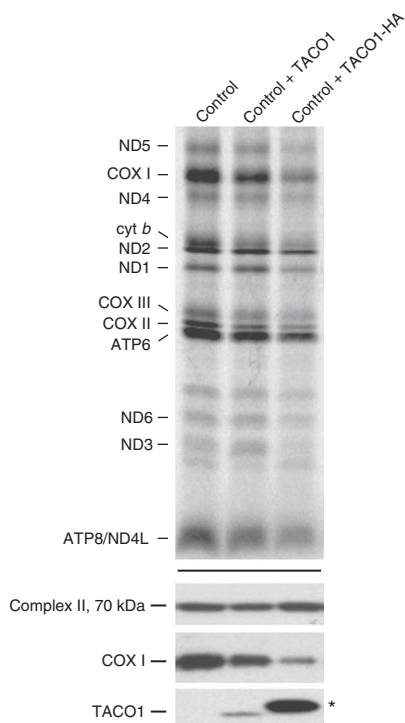


Figure 6 High levels of TACO1 or TACO1-HA expression depress mitochondrial translation in control fibroblasts. Top, pulse labeling of mitochondrial polypeptides. ND, subunits of complex I; COX, subunits of complex IV; cyt *b*, subunit of complex III; ATP, subunits of complex V. Bottom, the overexpression of TACO1 protein was confirmed by immunoblotting. An asterisk (*) denotes the TACO1-HA protein. The 70-kDa subunit of complex II was used as a loading control.

Fig. 6b). These data indicate that the protein encoded by YGR021w is not essential for the synthesis of full-length Cox1p or for respiratory competency in yeast. Analysis of patterns of coexpression for YGR021w using the SPELL algorithm⁵, however, shows a strong enrichment for factors involved in mitochondrial translation in yeast, suggesting that YGR021w may have some nonessential role in mitochondrial translation.

To our knowledge, TACO1 is the first specific mitochondrial translational activator identified in mammals. As mammalian mitochondrial mRNAs lack significant 5' UTRs³, most yeast genes involved in the translation of the mitochondrially encoded proteins lack mammalian homologs⁶. To date, one distant human homolog (LRPPRC) of the yeast translational activator Pet309 has been reported⁷. Both proteins contain PPR motifs, consisting of degenerate 35-amino-acid sequences that form antiparallel alpha helices, and which are thought to be involved in post-transcriptional mRNA metabolism, especially in mitochondria and chloroplasts^{8,9}. Mutations in LRPPRC lead to isolated COX deficiency in French-Canadian individuals with Leigh syndrome⁷. The protein is reported to be involved in the stabilization of the mRNAs for both COX I and COX III in mammals, without directly affecting their translation; however, the molecular mechanism remains unknown¹⁰.

TACO1 is clearly necessary for the efficient translation of COX I, as only a small amount of full-length polypeptide is synthesized in a null background in which the steady-state levels of COX I mRNA are normal. We envision three possible mechanisms. TACO1 might act by securing an accurate start of COX I translation, by stabilizing the elongating polypeptide and ensuring completion of its translation,

or by interacting with the peptide release factor, ensuring that the polypeptide does not dissociate from the ribosome until synthesis is complete.

TACO1 is conserved through bacteria, but most of the homologous sequences, all of which contain the so-called DUF28 domain, are annotated as hypothetical proteins. Recently, a DUF28 family member PmpR (from *Pseudomonas aeruginosa*) has been shown to be involved in a negative regulation of the quorum-sensing response regulator gene by binding to an upstream promoter element¹¹. Another DUF28 family member, Aq1575, a hypothetical protein from the hyperthermophilic bacterium *Aquifex aeolicus* (32% identical, 52% similar to TACO1), has been crystallized⁴. The protein has a large cleft surrounded by three domains, one of which represents a novel protein fold, but no obvious active site or functional domain could be identified in the crystal structure. The predicted three-dimensional structure of TACO1 is markedly similar to that of the *A. aeolicus* homolog considering the evolutionary distance between them (**Supplementary Fig. 7** online). It is tempting to suggest that this ancient protein evolved as a specific translational activator in concert with the loss of the mitochondrial mRNA regulatory sequences that occurred with the extreme reduction in the size of the metazoan mitochondrial genome.

METHODS

Methods and any associated references are available in the online version of the paper at <http://www.nature.com/naturegenetics/>.

Accession codes. GenBank: *CCDC44*, NP 057444.

Note: Supplementary information is available on the Nature Genetics website.

ACKNOWLEDGMENTS

We acknowledge the contribution of the individuals who cared for the study subjects and the technical assistance of I. Kaus, S. Mueller-Ziermann and A. Zimmermann. We thank T. Johns for help with immunocytochemistry and the cell culture. This work was supported in part by a grant from the Canadian Institutes of Health Research to E.A.S. E.A.S. is an International Scholar of the Howard Hughes Medical Institute. R.H. is supported by the Deutsche Forschungsgemeinschaft HO 2505/2-1.

AUTHOR CONTRIBUTIONS

W.W. did the chromosome transfer, mutation analysis, subcellular localization and RNA immunoblotting analyses; H.A. did BN gel analyses, enzyme measurements, molecular modeling and helped write the manuscript; F.S. performed translation analyses; J.S. evaluated the index subject and affected children; B.S. evaluated the adult subjects; J.E.K. did the yeast studies; H.L. performed the linkage analysis; M.C. helped with the chromosome transfer studies; B.A.K. did the size exclusion experiments and helped with the yeast studies; R.H. performed the histological, biochemical and genetic investigation of the index subject and family members; E.A.S. designed the study and wrote the final manuscript.

Published online at <http://www.nature.com/naturegenetics/>

Reprints and permissions information is available online at <http://npg.nature.com/reprintsandpermissions/>

1. Taylor, R.W. & Turnbull, D.M. Mitochondrial DNA mutations in human disease. *Nat. Rev. Genet.* **6**, 389–402 (2005).
2. Naithani, S., Saracco, S.A., Butler, C.A. & Fox, T.D. Interactions among COX1, COX2, and COX3 mRNA-specific translational activator proteins on the inner surface of the mitochondrial inner membrane of *Saccharomyces cerevisiae*. *Mol. Biol. Cell* **14**, 324–333 (2003).
3. Montoya, J., Ojala, D. & Attardi, G. Distinctive features of the 5'-terminal sequences of the human mitochondrial mRNAs. *Nature* **290**, 465–470 (1981).
4. Shin, D.H., Yokota, H., Kim, R. & Kim, S.H. Crystal structure of conserved hypothetical protein Aq1575 from *Aquifex aeolicus*. *Proc. Natl. Acad. Sci. USA* **99**, 7980–7985 (2002).
5. Hibbs, M.A. *et al.* Exploring the functional landscape of gene expression: directed search of large microarray compendia. *Bioinformatics* **23**, 2692–2699 (2007).
6. Fontanesi, F., Soto, I.C., Horn, D. & Barrientos, A. Assembly of mitochondrial cytochrome *c*-oxidase, a complicated and highly regulated cellular process. *Am. J. Physiol. Cell Physiol.* **291**, C1129–C1147 (2006).

7. Mootha, V.K. *et al.* Identification of a gene causing human cytochrome *c* oxidase deficiency by integrative genomics. *Proc. Natl. Acad. Sci. USA* **100**, 605–610 (2003).
8. Lurin, C. *et al.* Genome-wide analysis of *Arabidopsis* pentatricopeptide repeat proteins reveals their essential role in organelle biogenesis. *Plant Cell* **16**, 2089–2103 (2004).
9. Delannoy, E., Stanley, W.A., Bond, C.S. & Small, I.D. Pentatricopeptide repeat (PPR) proteins as sequence-specificity factors in post-transcriptional processes in organelles. *Biochem. Soc. Trans.* **35**, 1643–1647 (2007).
10. Xu, F., Morin, C., Mitchell, G., Ackerley, C. & Robinson, B.H. The role of the LRPPRC (leucine-rich pentatricopeptide repeat cassette) gene in cytochrome oxidase assembly: mutation causes lowered levels of COX (cytochrome *c* oxidase) I and COX III mRNA. *Biochem. J.* **382**, 331–336 (2004).
11. Liang, H., Li, L., Dong, Z., Surette, M.G. & Duan, K. The YebC family protein PA0964 negatively regulates the *Pseudomonas aeruginosa* quinolone signal system and pyocyanin production. *J. Bacteriol.* **190**, 6217–6227 (2008).

ONLINE METHODS

Subjects. The index subject is the fifth child of healthy consanguineous Turkish parents (**Supplementary Fig. 1**, V:5); three of the eight siblings are also affected (V:3; V:7; V:8) and five are healthy. One of the subject's five cousins (V:10; both parents are siblings of the parents of the index subject) is also affected. The index subject developed normally till 5 years of age. From this time his gait became unstable and his active speech worsened; however, his comprehension was relatively well preserved. The first detailed neurological examination at 10 years of age indicated that the subject was a small, thin, and dystrophic child (weight and height under the third percentile). Examination of cranial nerves revealed bilateral optic atrophy with otherwise normal eye movements, no ptosis or nystagmus, decreased mimic, bilateral facial weakness, prominent dysarthria and mild dysphagia. He had a spastic tetraparesis with increased deep tendon reflexes and Achilles clonus. He was able to sit without help, but was unable to stand or walk. Sensory symptoms and ataxia were not noted. Cognitive functions showed mild mental retardation.

Laboratory analysis showed increased serum lactate (4.1 mmol/l, normal <2 mmol/l), CSF lactate (3.2 mmol/l, normal <2 mmol/l) and pyruvate (1.6 mg/dl, normal <0.7 mg/dl). Other laboratory tests including CSF protein were normal.

Brain magnetic resonance imaging (MRI) showed bilateral, symmetric hyperintense lesions of the basal ganglia, typical for Leigh syndrome on T2/FLAIR sequences. Multiple hyperintense lesions in both frontal subcortical areas and in the subcortical region of the hemispheres were also present. Brainstem and cerebellum were normal.

A muscle biopsy at 10 years of age showed a few hypotrophic fibers and a generalized COX deficiency in all muscle fibers. No ragged red fibers or succinate dehydrogenase hyper-reactive fibers were noted. Biochemical analysis of the respiratory chain enzyme complexes I–IV and pyruvate dehydrogenase in skeletal muscle showed a severe isolated COX deficiency with approximately 15% residual activity of the enzyme; the activities of the other enzymes were within normal range.

The subject's siblings V:3, V:7, V:8 and cousin V:10 also presented with similar clinical symptoms, although the age of onset varied (16, 15, 4 and 14 years, respectively). They are all of thin, small stature, with variable neurological presentation including bilateral optic atrophy, spastic tetraparesis, dystoniiform movements, blurred speech and mild cognitive deficit. Notably, the affected girls showed a milder phenotype with preserved ambulation into the twenties, suggesting that sex-specific factors may influence the phenotype. In all four cases brain MRI showed bilateral, symmetric hyperintense lesions of the basal ganglia, typical for Leigh syndrome, with variable severity.

Human studies. We obtained informed consent from all investigated family members, and the research studies were approved by the institutional review board of the Montreal Neurological Institute and the Ludwig-Maximilians-University, Munich, Germany (Nr.084/00).

Cell lines. Primary cell lines were established from subject skin fibroblasts. The subject and control cell lines were immortalized by transduction with a retroviral vector expressing the HPV-16 E7 gene plus a retroviral vector expressing the catalytic component of human telomerase (hert)¹². The fibroblasts and HEK 293 line were grown at 37 °C in an atmosphere of 5% CO₂ in high-glucose DMEM supplemented with 10% FBS.

Enzyme activity measurements. Spectrophotometric assays of whole cell fibroblast extracts, or crude mitochondrial pellets from yeast, were used to measure enzyme activities. We normalized COX activity to citrate synthase activity and determined specific activity by protein content as described^{13,14}. Protein concentration was measured by the Bradford assay.

Electrophoresis and immunoblotting. Blue-Native PAGE was used to separate samples in the first dimension on 6–15% or 8–12% polyacrylamide gradient gels, as previously described¹⁵. Mitoplasts were prepared from fibroblasts by treatment with 0.8 mg of digitonin/mg of protein and solubilized with 1% lauryl maltoside; 20 µg of the solubilized proteins were used for electrophoresis. For the two-dimensional analysis, the BN-PAGE/SDS-PAGE was done as previously described¹⁴. Individual structural subunits of complexes I, II, III, IV and V were detected by immunoblot analysis using commercially available

monoclonal antibodies (Molecular Probes), except for complex I, where a polyclonal antibody against subunit ND1 (a gift of A. Lombes, INSERM U582, Hôpital de La Salpêtrière, Paris) was used.

We used SDS-PAGE to separate denatured whole cell extracts or isolated mitochondria using 12% polyacrylamide gels followed by immunoblot analysis with indicated antibodies. The antibody against EFTu/Ts was a gift of L. Sprenull (University of North Carolina, Chapel Hill).

Pulse labeling of mitochondrial translation products. *In vitro* labeling of mitochondrial translation products was conducted as previously described¹⁶. Briefly, cells were pulse-labeled for 60 min at 37 °C in methionine/cysteine-free DMEM containing 200 µCi/ml of a [³⁵S]methionine/cysteine mix (Perkin Elmer) and 100 µg/ml of either emetine or anisomycin. The cells were chased for 10 min (PULSE) or 17.5 h (CHASE) in regular DMEM. For chase studies, cells were incubated for 23 h in 40 µg/ml chloramphenicol before labeling. Total cellular protein (50 µg) was resuspended in loading buffer containing 93 mM Tris-HCl, pH 6.7, 7.5% glycerol, 1% SDS, 0.25 mg bromophenol blue/ml and 3% mercaptoethanol, sonicated for 3–8 s, loaded and run on 15–20% polyacrylamide gradient gels. The labeled mitochondrial translation products were detected through direct autoradiography.

RNA blot analysis. We isolated RNA from subject and control fibroblasts using the RNeasy Kit (Qiagen). Ten micrograms of total RNA were separated on a denaturing MOPS/formaldehyde agarose gel and transferred to a nylon membrane. We labeled 300- to 500-bp-long PCR products of individual mitochondrial genes with [α -³²P]-dCTP (GE Healthcare) using the MegaPrime DNA labeling kit (GE Healthcare). Hybridization was conducted according to the manufacturer's manual using ExpressHyb Hybridization Solution (Clontech) and the radioactive signal was detected using the Phosphorimager system.

Microcell-mediated chromosome transfer. Immortalized subject skin fibroblasts were fused with microcells carrying the q-arm of human chromosome 17 tagged with the hygromycin resistance gene, isolated from the B78MC57 mouse cell line^{17,18} by microcell-mediated chromosome transfer¹⁹.

Chromosome copy number analysis. The chromosome copy number was determined in rescuing and nonrescuing clones using SNP Mapping GeneChip Nsp 250 k Array (Affymetrix). This service was done by The Centre for Applied Genomics, Hospital for Sick Children, Toronto. The data were analyzed using the Copy Number Analysis Tool of GCOS Client software (Affymetrix).

Mutation detection. We isolated total RNA from subject and control skin fibroblasts using RNeasy Kit (Qiagen). TACO1 cDNA was amplified by using OneStep RT-PCR kit (Qiagen) and the gel-purified PCR fragments were used for direct sequencing. Total genomic DNA from controls, subject fibroblasts and blood from family members was isolated using DNeasy Kit (Qiagen). Primers specific for exon 3 of the TACO1 gene were used to amplify the DNA, followed by either digestion with MwoI or direct sequencing.

cDNA constructs and virus production and infection. Retroviral vectors containing the cDNA sequence of COX assembly factors (*COX11*, *COX16*, *COX17*, *OXA1*, *SCO1*, *SCO2*, *PET191*, *SURF1*, *OXA2*, *COX10*, *COX15.1*, *COX19*, *COX23* and *COX15.2*) were created with the Gateway Cloning system (Invitrogen) as previously described²⁰. cDNAs from the individual genes were amplified by OneStep RT-PCR (Qiagen) using specific primers modified for cloning into Gateway vectors, except for TACO1, where the cDNA (Open Biosystems, clone ID 4099917) in the Gateway modified vector pOTB7 was used. The PCR constructs were cloned into Gateway-modified retroviral expression vectors pLXSH or pBabe. For the C-terminal HA-tagged TACO1 (*TACO1-HA*), TACO1 cDNA was amplified using specific primers, cloned into pCR2.1-TOPO vector (Invitrogen), digested with EcoRI and cloned directly into EcoRI site of pBabe. We confirmed the fidelity of cDNA clones by DNA sequencing. Retroviral constructs were transiently transfected into the Phoenix packaging cell line using the HBS/Ca₃(PO₄)₂ method (see URLs section below). Subject and control fibroblasts were infected 48 h later by exposure to virus-containing medium in the presence of 4 µg/ml of polybrene as described²¹.

TACO1 antibody production. A polyclonal antibody against two peptides (Ac-IKGPKDVERSRIFSKLC-amide and Ac-LEFIPNSKVQLAEPDLEQAAC-

amide) from the human TACO1 protein was prepared by 21st Century Biochemicals (Marlboro, Massachusetts). Crude serum and affinity purified antibodies were tested on cell lines overexpressing TACO1 protein and detected a band of approximately 28 kDa. The C-terminal affinity-purified antibody was used for further experiments.

Yeast strains. Yeast strains BY4741p⁺, Y1236p⁺, ygr021wΔ and shy1Δ were obtained from the yeast genome deletion collection (see URLs section below). All strains were grown in standard media at 30 °C, with vigorous shaking for liquid cultures. For time-course experiments, we grew cells in either YPGal or YPGly (1% yeast extract, 2% peptone, and either 2% galactose or 3% glycerol, respectively) and monitored their growth over the course of 46 h by OD₆₀₀ readings. For respiratory competency experiments, yeast strains were grown on YEFD plates (1% yeast extract, 2% tryptone/peptone, 2% glucose) into colonies and covered with a 2,3,5-triphenyltetrazolium (TTC) (Sigma) overlay²².

Yeast translation assay. Mitochondrial protein synthesis was assessed as previously described²³, with certain modifications. Cells were grown to a maximum OD₆₀₀ of 1.0 in 3ml of methionine dropout media containing either 2% galactose or 3% glycerol. Cells were labeled with [³⁵S]methionine/cysteine mix for 20 min. After termination of the labeling reaction (including the addition of the NaOH/β-mercaptoethanol/PMSF solution), mitochondrial proteins were precipitated by the addition of 100% TCA to a final concentration of 15% and incubated on ice for 10 min. Samples were centrifuged and the pellet washed three times with cold acetone, followed by denaturation in 50 μl Laemmli SDS-PAGE loading buffer. Samples were separated on a 17.5% polyacrylamide gel.

Mitochondrial isolation and localization experiments. Fibroblasts were resuspended in ice-cold 250 mM sucrose/10 mM Tris-HCl/1 mM EDTA (pH 7.4) and homogenized with 10 passes through a pre-chilled, zero clearance homogenizer (Kimble/Kontes). We centrifuged samples twice for 10 min at 600g to obtain a postnuclear supernatant. Mitochondria were pelleted by centrifugation for 10 min at 10 000g, and washed once in the same buffer. Mitochondria were either sonicated or further extracted with 100 mM alkaline carbonate as previously described¹², and the relevant fractions were analyzed by SDS-PAGE.

Immunocytochemistry. HEK293 cells were plated on coverslips and transfected with TACO1-HA cDNA in pCR2.1-TOPO vector using Lipofectamine (Invitrogen). Twenty-four hours post-transfection, the cells were paraformaldehyde-fixed, solubilized by Triton X-100 and stained using antibodies to hemagglutinin (Sigma) and cytochrome *c* (BD Pharmingen). Secondary antibodies ALEXA488 (anti-mouse) and ALEXA 594 (anti-rabbit) (Molecular Probes) were used for immunofluorescence detection.

Size exclusion chromatography. We separated soluble proteins from mitochondrial detergent extracts on a Tricorn Superdex 200 10/30 HR column (GE Healthcare) as described²⁴ and determined elution profiles by immunoblot analysis using antibodies against TACO1, EFTs and EFTu.

Molecular modeling. The three-dimensional structure of TACO1 was modeled on the crystal structure of Aq1575 (ref. 4) homolog using the I-TASSER server^{25–27} and viewed with Swiss-MODEL using the Swiss-Pdb Viewer²⁸.

URLs. Phoenix-Helper dependent protocol, http://www.stanford.edu/group/nolan/protocols/pro_helper_dep.html; Saccharomyces Genome Deletion Project, http://www-sequence.stanford.edu/group/yeast_deletion_project/deletions3.html; Swiss PDB viewer, <http://www.expasy.org/spdbv/>.

- Yao, J. & Shoubridge, E.A. Expression and functional analysis of *SURF1* in Leigh syndrome patients with cytochrome *c* oxidase deficiency. *Hum. Mol. Genet.* **8**, 2541–2549 (1999).
- Capaldi, R.A., Marusich, M.F. & Taanman, J.W. Mammalian cytochrome-*c* oxidase: characterization of enzyme and immunological detection of subunits in tissue extracts and whole cells. *Methods Enzymol.* **260**, 117–132 (1995).
- Antonicka, H. *et al.* Mutations in COX10 result in a defect in mitochondrial heme A biosynthesis and account for multiple, early-onset clinical phenotypes associated with isolated COX deficiency. *Hum. Mol. Genet.* **12**, 2693–2702 (2003).
- Klement, P., Nijtmans, L.G., Van den Bogert, C. & Houstek, J. Analysis of oxidative phosphorylation complexes in cultured human fibroblasts and amniocytes by blue-native-electrophoresis using mitoplasts isolated with the help of digitonin. *Anal. Biochem.* **231**, 218–224 (1995).
- Boulet, L., Karpati, G. & Shoubridge, E.A. Distribution and threshold expression of the tRNA(Lys) mutation in skeletal muscle of patients with myoclonic epilepsy and ragged-red fibers (MERRF). *Am. J. Hum. Genet.* **51**, 1187–1200 (1992).
- Gagnon, A., Ripeau, J.S., Zvieriev, V. & Chevrette, M. Chromosome 18 suppresses tumorigenic properties of human prostate cancer cells. *Genes Chromosom. Cancer* **45**, 220–230 (2006).
- Cuthbert, A.P. *et al.* Construction and characterization of a highly stable human: rodent monochromosomal hybrid panel for genetic complementation and genome mapping studies. *Cytogenet. Cell Genet.* **71**, 68–76 (1995).
- Zhu, Z. *et al.* *SURF1*, encoding a factor involved in the biogenesis of cytochrome *c* oxidase, is mutated in Leigh syndrome. *Nat. Genet.* **20**, 337–343 (1998).
- Antonicka, H. *et al.* Mutations in COX15 produce a defect in the mitochondrial heme biosynthetic pathway, causing early-onset fatal hypertrophic cardiomyopathy. *Am. J. Hum. Genet.* **72**, 101–114 (2003).
- Lochmuller, H., Johns, T. & Shoubridge, E.A. Expression of the E6 and E7 genes of human papillomavirus (HPV16) extends the life span of human myoblasts. *Exp. Cell Res.* **248**, 186–193 (1999).
- Barclay, B.J. *et al.* A rapid assay for mitochondrial DNA damage and respiratory chain inhibition in the yeast *Saccharomyces cerevisiae*. *Environ. Mol. Mutagen.* **38**, 153–158 (2001).
- Barrientos, A., Korr, D. & Tzagoloff, A. Shy1p is necessary for full expression of mitochondrial COX1 in the yeast model of Leigh's syndrome. *EMBO J.* **21**, 43–52 (2002).
- Kaufman, B.A. *et al.* The mitochondrial transcription factor TFAM coordinates the assembly of multiple DNA molecules into nucleoid-like structures. *Mol. Biol. Cell* **18**, 3225–3236 (2007).
- Wu, S., Skolnick, J. & Zhang, Y. Ab initio modeling of small proteins by iterative TASSER simulations. *BMC Biol.* **5**, 17 (2007).
- Zhang, Y. I-TASSER server for protein 3D structure prediction. *BMC Bioinformatics* **9**, 40 (2008).
- Zhang, Y. Template-based modeling and free modeling by I-TASSER in CASP7. *Proteins* **69**(Suppl 8), 108–117 (2007).
- Guex, N. & Peitsch, M.C. SWISS-MODEL and the Swiss-PdbViewer: an environment for comparative protein modeling. *Electrophoresis* **18**, 2714–2723 (1997).